11th INTERNATIONAL CONFERENCE ON CONTACT MECHANICS AND WEAR OF RAIL/WHEEL SYSTEMS (CM2018)
DELFT, THE NETHERLANDS, SEPTEMBER 24-27, 2018

LOCAL PLASTICITY MODELLING AND ITS INFLUENCE ON WHEEL-RAIL FRICTION

C.D. van der Wekken [1,*], E.A.H. Vollebregt [1]

[1] VORtech CMCC, Westlandseweg 40d, 2624 AD Delft

[*] E-mail: niels.vanderwekken@vortech.nl

Abstract: Friction is an interesting topic because of its important influence in wear during wheel-rail contact and vehicle system dynamics. To be able to reduce wear while maintaining safe and fast operation of the train network a better understanding of friction and the role of friction modifiers is key. Inspired by the approaches of Tomberger [1] and Meierhofer [2] in this paper we will present a model to calculate the amount of local plastic deformation occurring in rolling contact. This model is compatible with the variational theory and has been implemented in the CONTACT software.

Keywords: Plastic deformation; friction; traction; rolling contact; half-space assumption; third body layer.

1. Introduction

Friction is an important topic because of its influence on vehicle dynamics and wear in the wheel-rail system. To reduce wear, while maintaining safe and fast operation of railways, a better understanding of friction and friction modifiers is key. However, with increased research and measurements on friction [3, 4], it becomes ever more clear that the underlying physics are not well understood. The main thing that is clear is that "Coulomb friction" works as a first estimate only and more detailed modeling is necessary to capture the underlying effects.

Supported by a programme of the US Federal Railroad Administration, VORtech CMCC is developing physics-based sub-models for friction related phenomena for the CONTACT software [5]. Inspired by the works of Tomberger et al. [1] and Meierhofer et al. [2] these sub-models are: the wheel and rail surface temperatures, the surface roughness, the presence of fluids and friction modifiers, and the effects of plastic deformation in the near surface layer. This paper concentrates on the last aspect, incorporating "local plasticity" in CONTACT. A sub-model is being developed to capture the effects of plastic deformation and of the accompanying third body layer where this plastic deformation occurs.

A local plasticity model has been developed. Section 2 describes different approaches others have taken, followed by what will form the basis for our model. Section 3 describes the mathematical details of our model. After incorporating this model into Kalker's complete contact theory test runs are performed. In Section 4 the results, including the influence of plasticity on the coefficient of traction, are compared to results obtained by Meierhofer [2]. Finally, our conclusions can be found in Section 5.

2. Modeling approach

Six et al. [6, 7] present the division of plastic phenomena in "global" and "local" plasticity. Plasticity is qualified as "global" if it occurs on the range of millimeters, while local plasticity occurs in the range of microns. Next to the typical size of their effect, global plasticity has a short shakedown cycle. After some initial deformation of fresh material, the material will harden and not deform further. Local plasticity, called "tribological plasticity" in [7], is described as the plasticity that occurs on the scale of the materials asperities. This is an ongoing process. The asperities deform plastically, are removed from the surface by wear, and after this, new asperities will wield the contact forces, exposing the new asperities to wear.

Following the distinction of global and local plasticity of Six there are two different scenarios to consider. First there is the global plastic deformation. Different models exist to deal with this case, for example the approach by Sebès [8] or the one by Hauer [9]. These models dealing with changing of the profile shapes, however, do not give insight in the effects of plastic deformation and the appearance of a third body layer on the friction during rolling. To achieve this, it is necessary to look at a local plasticity model, one such a model is described by Meierhofer [2]. Our approach uses the ideas of Meierhofer's model, based on a simplification of the stress-strain curve by Hou [10], although the details are worked out differently.

Hou's simplification of the stress-strain curve starts with a fully elastic linear relation between the shear stress and the shear strain, through the (elastic) shear modulus G. Then once the yield point is reached plastic deformation will start to occur, and the shear stress and strain will relate through another linear relation, with a new (plastic) shear modulus k. This is schematically represented in Figure 1.

The model used by Meierhofer starts from a parabolic solution to the normal problem. Tangentially, the bulk materials are described as linearly elastic, using a polynomial series approach for plane strain situations.

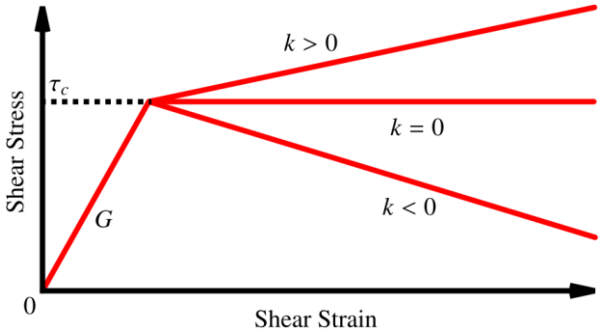

Figure 1: *Simplified stress-strain curves proposed by Hou [10], relating shear stress τ to shear strain γ by elastic (G) and plastic (k) regimes, with strain-hardening ($k > 0$), elastic-perfectly plastic ($k = 0$) and strain-weakening characteristics ($k < 0$).*

The characteristic of Figure 1 is added through a third body layer based on independent brushes of sprints, like Kalker's simplified theory [11] (FASTSIM), with varying stiffness proportional to G or k depending on the actual value of τ.

Meierhofer's local plasticity formulation appears to be incompatible with the variational theory [12] as implemented in CONTACT. The main reason is that the tractions τ or p are used as primary unknowns, for which the characteristic of Figure 1 must be inverted. The relationship then becomes multi-valued if $k = 0$ or $k < 0$. Even if the tractions are known at all places, the displacements still cannot be computed.

In the context of the Extended CONTACT model [13], plastic effects will be captured in an infinitesimal third body layer while the bulk material of the rail and wheel are still assumed to be elastic half-spaces. This thin layer will therefore not be an extra layer with specified thickness in the calculations, but will represent the layer where tangential plastic deformation in the surfaces of the two bulk bodies occurs. This results in a local plasticity model that is compatible with the current implementation of the Extended CONTACT software.

A model is constructed for tangential plastic deformation. An intuitive idea of how this works out is given in Figures 2 to 6. This shows how the relative surface displacements may be accommodated, for increasing amounts of rigid slip w. Initially, w is accounted for by elastic deformation u_{el}. Plastic deformation u_{pl} arises if the stress needed grows up to the yield limit τ_c, and slip s arises if the local Coulomb maximum μp_n is reached. This shows that rigid slip (creepage) may be accommodated in three different ways, using elastic deformation, plastic deformation and true slip. The mixture in which they occur depends on the parameters of the problem, like the material rigidity G, yield limit τ_c, the pressure p_n, and the coefficient of friction μ.

3. Model implementation

Following the model by Hou [10] we use a constant modulus of rigidity G in the elastic regime and a different, constant modulus of rigidity k in the plastic regime. This means that in the plastic regime, the relation between the total traction and total displacements will be linear again. The actual value of this parameter k should be determined experimentally, this is out of the scope of our work, where we focus on the theoretical model only.

Figure 2: *At low creepage, the surfaces' relative displacement can be accommodated easily by elastic displacement.*

Figure 3: *Surface tractions τ increase in proportion to the elastic displacement u^{el}. At some amount of rigid slip w, the required traction τ just reached the yield point τ_c.*

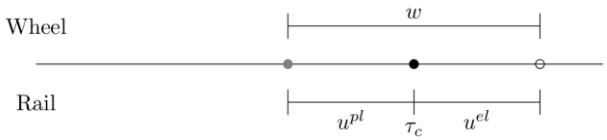

Figure 4: *The creep is a bit larger than in Figure 3. Because there is no elastic deformation anymore beyond the yield point, the additional creeping is compensated for through plastic deformation. The yield limit τ_c can change depending on the value of k.*

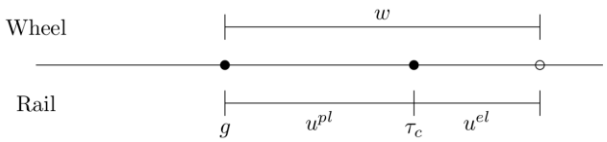

Figure 5: *The rigid slip w is chosen such that the material hardens up to the original traction bound, $\tau_c = g = \mu p_n$.*

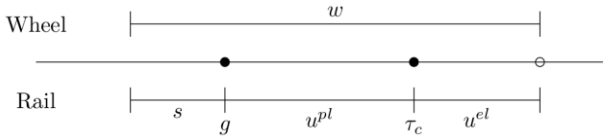

Figure 6: *With rigid slip w requiring tractions larger than the traction bound g, there will be actual slip s next to elastic and plastic deformation.*

One main equation in rolling contact is the so-called "slip equation":

$$\mathbf{s}_{rel} = \mathbf{w}_{rel} + \frac{1}{V}\frac{\mathrm{D}\mathbf{u}}{\mathrm{D}t}. \qquad (1)$$

Here $\mathbf{s}_{rel}$ is the actual (micro-) slip relative to the rolling velocity V, that is linked to the rigid slip $\mathbf{w}_{rel}$, imposed by creepage, and to material deformation: $\mathrm{D}\mathbf{u}/\mathrm{D}t$. The displacements are written as the sum of elastic and plastic displacements:

$$\mathbf{u} = \mathbf{u}_{tot} = \mathbf{u}_{el} + \mathbf{u}_{pl}. \qquad (2)$$

Using the halfspace approach, the elastic displacements are found with Green's functions, aggregating the effect of the tractions $\mathbf{p}(\mathbf{y})$:

$$\mathbf{u}_{el}(\mathbf{x}) = \iint_C \mathbf{A}(\mathbf{x},\mathbf{y})\mathbf{p}(\mathbf{y})dS. \qquad (3)$$

Micro-slip is supposed to occur where the traction bound is reached, which is modelled using Coulomb friction. This sets the local traction bound g as the product of normal pressure p_n with μ, the local coefficient of friction.

$$g = \mu p_n. \tag{4}$$

Plasticity is introduced where the tractions reach the current yield stress τ_c, which depends on the amount of plastic deformation that occurred previously. Inverting the stress-strain relationship of Figure 1, this is obtained as:

$$\tau_c = \tau_{c0} + \tilde{k} u^*_{pl}, \tag{5}$$

where $\tilde{k} = Gk/(G-k)$, and where:

$$u^*_{pl} = \int_t \left\| \frac{\mathrm{D}\mathbf{u}_{pl}}{\mathrm{D}t} \right\| dt. \tag{6}$$

This aggregates the total plastic deformation experienced by the material in absolute sense, irrespective of the direction in which the deformation occurs. Thereby, deforming in one direction does not cancel previous deformation in the opposite direction, in line with the concepts of material fatigue.

The final part of the model consists of the contact conditions, that specify how the tractions $\mathbf{p}$, micro-slip $\mathbf{s}$ and plastic deformation $\mathbf{u}_{pl}$ are related. Four different regimes are considered for the exterior area E, elastic adhesion H, plastic adhesion P, and slip area S:

$$\text{in } E: \quad \|\mathbf{p}\| = 0, \qquad \mathbf{s} \text{ free}, \qquad \frac{\mathrm{D}\mathbf{u}_{pl}}{\mathrm{D}t} = \mathbf{0}, \tag{7}$$

$$\text{in } H: \quad \|\mathbf{p}\| \le \min(g, \tau_c), \qquad \mathbf{s} = \mathbf{0}, \qquad \frac{\mathrm{D}\mathbf{u}_{pl}}{\mathrm{D}t} = \mathbf{0}, \tag{8}$$

$$\text{in } S: \quad \|\mathbf{p}\| = g \le \tau_c, \qquad \mathbf{s} // \mathbf{p}, \qquad \frac{\mathrm{D}\mathbf{u}_{pl}}{\mathrm{D}t} = \mathbf{0}, \tag{9}$$

$$\text{in } P: \quad \|\mathbf{p}\| = \tau_c < g, \qquad \mathbf{s} = \mathbf{0}, \qquad \frac{\mathrm{D}\mathbf{u}_{pl}}{\mathrm{D}t} // \mathbf{p}. \tag{10}$$

These equations reduce to the variational theory when $\tau_c = \infty, \mathbf{u}_{pl} = 0$: the exterior area is free of traction, no slip occurs unless the traction bound is reached, and where slip occurs, this is in the direction opposite to the tractions. The extension concerns the introduction of a yield limit. This provides a different upper bound for the elastic adhesion regime. Once the yield point is reached, plastic deformation occurs. In this case, plastic deformation itself may alter the yield limit, as described in Equations (5) and (6). On the one hand, this makes the system stronger non-linear than the original model. On the other hand, this resolves most of the ambiguities that could occur when $g = \tau_c$.

4. Results

2D Carter testcase: The model of the previous paragraph is implemented in CONTACT for 2D situations. Figure 7 shows the results for the Carter testcase for a range of different values $k_{rel} = k/G$. In any case, material enters the contact area on the right with adhesion, $p_x < \min(g, \tau_c)$. The current yield limit τ_c then starts at the fresh yield value τ_{c0}. Tractions build up gradually until the yield limit is reached, that's lower than the traction bound g. The material then deforms plastically, the yield limit τ_c changing dependent on the value of k. Finally, the traction bound g lowers because of the pressures reducing. Slip is then found at the trailing end of the contact (left side), with no further plasticity and constant τ_c.

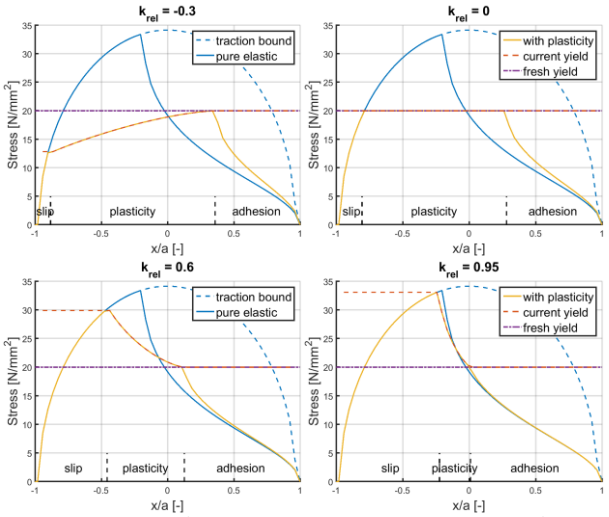

Figure 7: *Results of the extended model with local plasticity for the 2D Carter testcase, for* $k\_rel = k/G = -0.3, 0, 0.6,$ *and* 0.95.

The biggest plasticity area P is found at the lowest value of k_{rel}. This gives the lowest tractions on the left side of the contact area, increasing the tractions on the right. The plasticity area reduces when k_{rel} is increased further and further, with the tractions converging to those of the elastic case. Note that $\tilde{k} \to \infty$ as $k_{rel} \uparrow 1$, such that just a small bit of u^*_{pl} is needed in order to lift τ_c up to g.

Meierhofer testcase: The second testcase considered concerns the configuration as described by Meierhofer et al. [2]. This uses the input parameters as listed in Table 1. Two computations are performed, for creepages $\xi = 0.3$ and 1.0%. The results are shown in Figure 8, next to those obtained by Meierhofer et al.

Table 1 *Parameters used in the Meierhofer-testcase (Figure 8) and the computation of creep curves (Figure 9).*

Parameter	Symbol	Quantity
Elastic modulus of rigidity	G	$77519.4\ MPa$
Plastic modulus of rigidity	k	$3000\ MPa$
Initial yield strength	τ_{c0}	$200\ MPa$
Poisson's ratio	ν	0.29
Coefficient of friction	μ	0.5
Total normal force	F_0	$1323.6\ N/mm$

The figure shows that the results are generally in good agreement with each other, even though the two models are based on different computational approaches. Our model generally finds somewhat higher stresses, both in the purely elastic case and in the extended model where plasticity is included.

Note that Meierhofer's model starts from a parabolic pressure distribution, and uses a series expansion for the elastic displacements. Next, a third body layer is

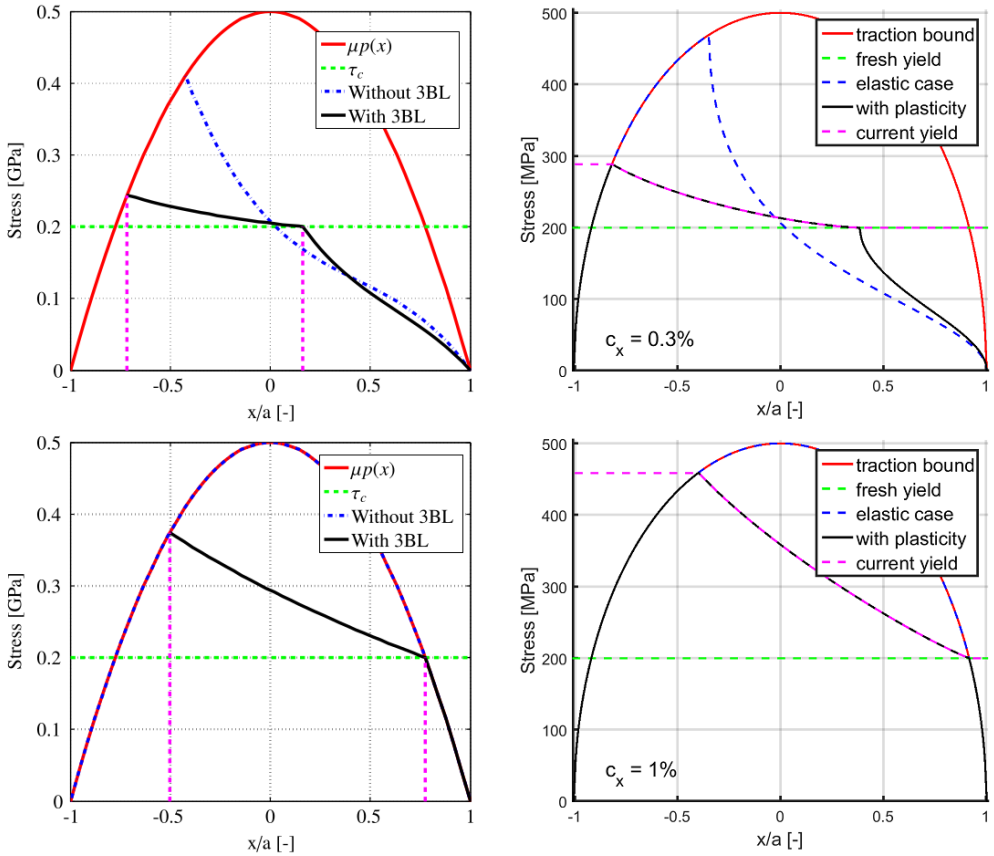

Figure 8: *Left: results from Meierhofer [2, Fig 7]. Right: results of the Extended CONTACT model. Parameters are given in Table 1. Top: creep $\xi = 0.3\%$, bot: $\xi = 1.0\%$.*

introduced of a finite thickness h, with a purely local relationship $u_{3bl}(x) = -h \cdot \tau(x)/m(x)$. This describes a spring with variable stiffness $m(x)$. One drawback of this spring is that it has no permanent plastic deformation, energy could be stored first and then be regained upon unloading.

Calculation of creep-force curves: The third test concerns the effect of local plasticity on the coefficient of traction, as shown in Figure 9. This shows the relative tangential force F_x/F_n as a function of creepage c_x. The initial yield value is $\tau_{c0} = 200\,MPa$ in the graph on the left, versus $\tau_{c0} = 350\,MPa$ on the right. The various lines in each graph are given for different values of the parameter k_{rel}.

The figure shows that local plasticity reduces the tangential forces compared to the elastic model. How this works out depends on the ratio $k_{rel} = k/G$. For $k_{rel} > 0$, the curves eventually tend to the original maximum μ, yet this happens slower and slower as k_{rel} is reduced. This relates to the situation of $k_{rel} = 0.95$ in Figure 7. When c_x is increased, the actual yield limit τ_c will be pushed up as well, until ultimately, the original tractions p_x are regained.

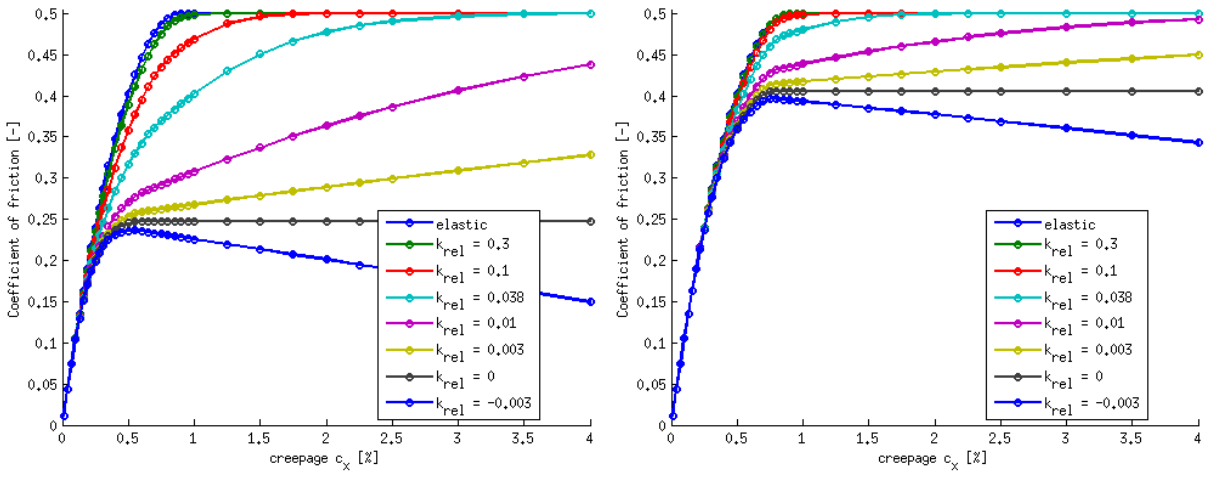

Figure 9: *Coefficient of traction as a function of the amount of creep. Parameters are given in Table 1. Left: $\tau_{c0} = 200\,MPa$, right: $\tau_{c0} = 250\,Mpa$.*

At $k_{rel} = 0$, the creep-force curves saturate at a lower maximum than the original maximum μ. This new maximum is seen to depend on the yield limit τ_{c0}. This is understood using the situation of $k_{rel} = 0$ in Figure 7. With plasticity, there's an effective traction bound $\min(g, \tau_{c0})$, i.e. the higher values of g are chopped off. This reduces the maximum F_x that may be delivered. This effect becomes stronger when τ_{c0} is reduced. Finally, at $k_{rel} < 0$, the creep-force curves are seen to approach the lower maximum of $k_{rel} = 0$ first, but then show a decreasing trend if c_x is increased further.

5. Conclusions and discussion

Previously, in CONTACT the assumption was made that all deformation was purely elastic. There is strong evidence of plastic deformation of the wheel and rail materials in the vicinity of the contacting surfaces. Part of this plasticity is termed "global", related to peak pressures due to non-conforming profiles. Another part termed "local plasticity" is concerned with the tangential shear stresses. It is hypothesised that this local plasticity continues to exist even after the surfaces are run in, and that it may alter the creep-force behaviour significantly.

The CONTACT model has been extended to account for this local plasticity. The existence of a tangential yield stress τ_c is postulated for this. It then becomes possible to increase the amount of stress beyond the initial yield stress by moving from the elastic domain into the plastic domain locally.

Plastic deformation $\delta\mathbf{u}_{pl}$ occurs in the direction of the tractions $\mathbf{p}$ where this yield stress is reached, much alike the occurrence of micro-slip $\mathbf{s}$ where the tangential traction bound $g = \mu p_n$ is reached for Coulomb friction. The tangential yield stress is postulated to change with the amount of accumulated plasticity u_{pl}^*, using the three simplified schemes of Hou et al. [10]: $k > 0,\ k = 0,\ k < 0$. This is expressed in a model of equalities and constraints in equations (2) – (10). This model is discretized and then solved rigorously by distinction of the possible regimes.

The new model deviates from the one by Meierhofer et al. in at least three different ways. Firstly, we allow for plasticity to occur in the wheel and rail surfaces instead of confining it to the third body layer. The quantity $\mathbf{u}_{pl}$ tells how much the opposing surfaces are displaced with respect to each other, without information on the vertical distributed of this. Secondly, the condition is added that $\delta\mathbf{u}_{pl} // \mathbf{p}$, to ensure that $\boldsymbol{u}_{pl}$ remains in tact upon relieving the stress, such that energy is lost by plastification. In the model by Meierhofer et al., the third body layer acts as a spring with variable stiffness that undoes "plastic deformation" when the stresses diminish. Energy may still be dissipated in their model, increasing the micro-slip $\mathbf{s}$ compared to the fully elastic situation. However, this is not guaranteed in situations with mixed creepage. Further, the energy is dissipated at the wrong place, affecting for instance the calculation of surface temperatures. A third difference between the two models concerns the method of discretization. The series of polynomial terms used by Meierhofer et al. is essentially restricted to 2D situations, whereas the grid used in CONTACT supports 3D situations also. Note that this is not yet worked out for the plasticity calculation.

Calculations with the new model show the robustness of the calculation of different regimes, over a wide range of k_{rel}, τ_{c0} and creepages ξ. The results of the model are largely similar to those of Meierhofer et al., truncating the tangential tractions $\mathbf{p}$ in regions with high pressures. This has a pronounced effect on the creep versus creep-force behavior, particularly at small values of k_{rel}. A much slower transition from the linear to the saturated regimes is obtained, resembling the results of twin-disc experiments presented in [2].

This results in a lower coefficient of traction. How much lower this coefficient is, and therefore if there is a significant difference to the elastic model depends on physical material parameters. Especially materials that experience little work hardening under plastic deformation are sensitive to loss of traction compared to the elastic model.

References

[1] C. Tomberger, P. Dietmaier, W. Sextro, and K. Six. *Friction in wheel-rail contact: a model comprising interfacial fluids, surface roughness and temperature.* Wear, 271: 2-12, 2011.

[2] A. Meierhofer, C. Hardwick, R. Lewis, K. Six, and P. Dietmaier. *Third body layer - experimental results and a model describing its influence on the traction coefficient.* Wear, 314: 148-154, 2014.

[3] H. Harrison. *The development of a low creep regime, hand-operated tribometer*. Wear, 265: 1526-1531, 2008.

[4] R.I. Popovici. *Friction in Wheel - Rail Contacts.* PhD thesis, University of Twente, The Netherlands, 2010.

[5] E.A.H. Vollebregt. *User guide for CONTACT, Rolling and sliding contact with friction.* Technical Report TR09-03, version 18.1, VORtech, 2018. See www.kalkersoftware.org.

[6] K. Six, A. Meierhofer, G. Müller, and P. Dietmaier. *Physical processes in wheel-rail contact and its implications on vehicle-track interaction.* Vehicle System Dynamics, 53(5): 635-650, 2015.

[7] K. Six, A. Meierhofer, G. Trummer, C. Bernsteiner, C. Marte, G Müller, B. Luber, P. Dietmaier, and M. Rosenberger. *Plasticity in wheel-rail contact and its implications on vehicle-track interaction.* Proceedings of the Institution of Mechanical Engineers, Part F: Journal of Rail and Rapid Transit, 231(5): 558-569, 2016.

[8] M. Sebès, L. Chevalier, J.B. Ayasse, and H. Chollet. *A fast simplified wheel-rail contact model consistent with perfectly plastic materials.* Vehicle System Dynamics, 50(9): 1453-1471, 2012.

[9] F. Hauer. *Die elasto-plastische Einglättung rauer Oberflächen und ihr Einfluss auf die Reibung in der*

Umformtechnik. PhD thesis, Friedrich-Alexander-Universität Erlangen-Nürnberg, 2014.

[10] K. Hou, J. Kalousek, and E. Magel. *Rheological model of solid layer in rolling contact.* Wear, 211: 134-140, 1997.

[11] J.J. Kalker. *A fast algorithm for the simplified theory of rolling contact.* Vehicle System Dynamics, 11: 1-13, 1982.

[12] J.J. Kalker. *Three-Dimensional Elastic Bodies in Rolling Contact*, volume 2 of Solid Mechanics and its Applications. Kluwer Academic Publishers, Dordrecht, Netherlands, 1990.

[13] E.A.H. Vollebregt. *Numerical modeling of measured railway creep versus creep-force curves with CONTACT.* Wear, 314: 87-95, 2014.